HIGH-FREQUENCY SCATTERING FROM A MUDDY SAND SEDIMENT WITH AN OVERLYING MUD LAYER.

Brian T. Hefner Applied Physics Laboratory, University of Washington, Seattle, WA, USA
Anatoliy Ivakin Applied Physics Laboratory, University of Washington, Seattle, WA, USA
Darrell R. Jackson Applied Physics Laboratory, University of Washington, Seattle, WA, USA

1 INTRODUCTION

While a significant amount of research has been conducted on the response of mines and munitions in sand sediments, the acoustic reponse of targets in muddy environments is not well understood. This lack of understanding exists despite the prevalence of this bottom type in very shallow water areas such as harbors and bays. This is largely due to the difficulty of collecting both acoustic measurements and sufficient environmental characterization to understand not only the acoustic response of the targets in the environment but the response of the sediment itself.

These challenges motivated the selection of the Bay Experiment (BayEx14) site which took place in St. Andrew's Bay in the spring of 2014 and was jointly sponsored by the US Office of Naval Research (ONR) and the Strategic Environmental Research and Development Program (SERDP). The experiment site was in 7 m of water and the seafloor consisted of a 10–15 cm thick mud layer on top of a sand/mud bottom. This sand/mud basement was rigid enough to support the placement of mechanical and electronic systems on the bottom and prevent the acoustic targets from sinking into the mud. This made it possible to deploy the suite of instruments that had been developed for previous experiments in areas with sand bottoms, such as the Sediment Acoustics Experiments in 1999 (SAX99)[1] and 2004 (SAX04)[2] and the more recent Target and Reverberation Experiment in 2013 (TREX13).[3]

The primary thrust of BayEx14 was to use synthetic aperture sonar to study target scattering in a sand/mud environment. In addition to these measurements, a second set of data was collected to look at mid and high-frequency backscattering from the seafloor in the absence of the targets. The goal of this work was to understand the dominant scattering mechanisms in this environment, how the introduction of the mud layer affects the scattering response, and to support the development of an acoustic seabed classification technique. To interpret the data and develop scattering models for this sediment, extensive environmental characterization was performed at this site as well. This paper presents the inversion and analysis of multibeam sonar data using the environmental characterization collected at the site.

2 MEASUREMENTS

2.1 MULTIBEAM SONAR

The experiment took place in the southeast arm of St. Andrew's Bay near Panama City Beach, Florida (Figure 1). A majority of the data was collected from May 8 to May 27 while the R/V Sharp was in a four-point moor at the experiment site. Instruments and acoustic systems deployed on the bottom were cabled to the ship which also acted as a platform for the deployment of divers to assist in the setup and operation of the equipment. Despite efforts by the divers to minimize contact with the seafloor, dive operations significantly disturbed the seafloor, artificially modifying the environment. In

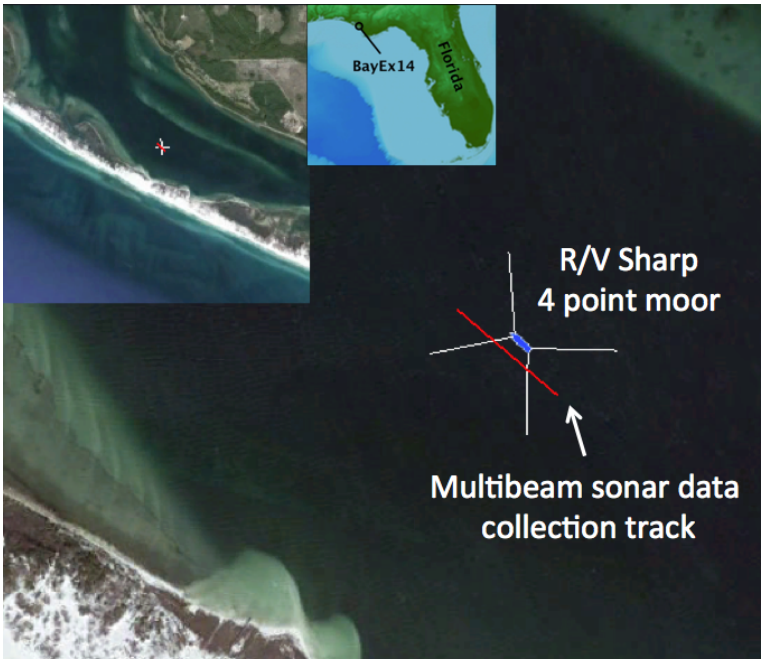

Figure 1: Location of the Moored R/V Sharp and the multibeam sonar data collection track.

anticipation of this disturbance, the multibeam sonar collected backscatter data prior to the arrival of the R/V Sharp at the experiment site.

The multibeam sonar used was a Teledyne-RESON 7125 which is usually operated at either 200 kHz or 400 kHz depending on the depth of the seafloor. The beam width at 200 kHz is 2 degrees along track and 1 degree across track. The beam width at 400 kHz is 1 degree along track and 0.5 degrees across track. The beams extend across a full swath-width of 140 degrees. For this work, the software used to run the 7125 was modified to operate at 20-25 kHz increments from 180 kHz to 420 kHz. The beam widths at each frequency varied between the two extremes at 200 and 400 kHz.

In typical bathymetric measurements using a multibeam sonar, only the timing and magnitude of the peak scattered signal is recorded for each beam. In this project, which seeks to develop a seabed classification technique, the full time series data was collected for each beam. To collect this time series data at the 11 frequencies of interest, a single 200 m long track was chosen to be the focus of the data collection. This track ran parallel to the subsequent orientation of the ship and passed to its southeast as indicated in Figure 1.

The data collected by the multibeam was then processed using an inversion technique developed over the course of several experiments including TREX13.[4] The ultimate goal of any seabed classification technique is to determine the intrinsic physical properties of the sediment such as density, sound speed, and porosity. As opposed to the empirical approaches used in other classification techniques, in the inversion used here the acoustic data collected with the multibeam was used to first obtain estimates of the interface scattering strength, volume scattering, and attenuation. These parameters are estimated by fitting a model for the echo intensity time series, as in.[5–8] This approach separates the interface and volume scattering, which is possible due to the high directivity of the multibeam sonar. The estimates of the interface scattering strength can then be used to estimate the roughness parameters and the impedance of the sediment. Further estimates of the sediment parameters such as porosity and density can be obtained by using these parameters with published empirical relationships.

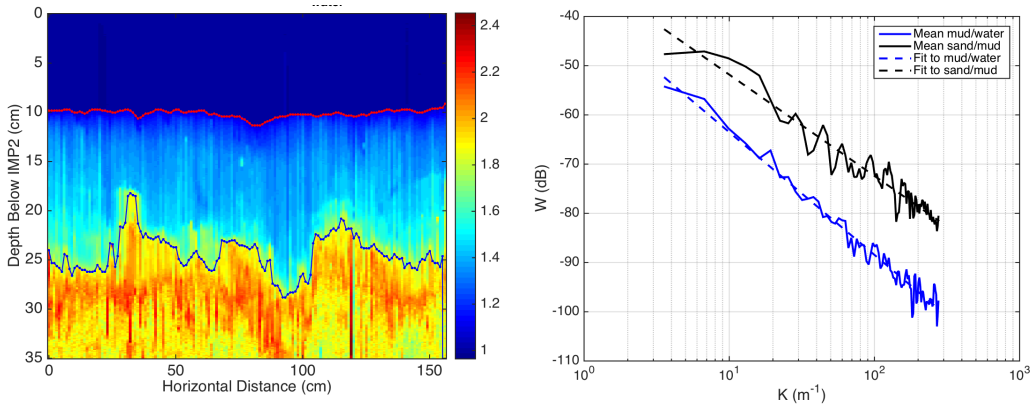

(a) (b)

Figure 2: (a) Formation factor measured by the IMP2 conductivity probe in St. Andrew's Bay. The red and black lines indicate the mud/water interface and the sand/mud interface respectively. (b) The roughness power spectra corresponding to the surfaces indicated in (a).

2.2 ENVIRONMENTAL CHARACTERIZATION

While the R/V Sharp was in a four-point moor, diver cores and conductivity data were collected in order to determine the sediment properties. This data was collected on the south side of the ship to coincide with the center of the MBES track. Two sets of diver cores were collected; one capturing only the mud layer and the other capturing only the sand/mud basement. Both sets were analyzed for porosity and density. For the mud layer, the density was $\rho_m = 1.26 \pm 0.06$ g/cm^3 and the porosity was $\beta_m = 81\% \pm 1\%$. The underlying sand had a density of $\rho_s = 2.10 \pm 0.02$ g/cm^3 and a porosity of $\beta_s = 40\% \pm 1\%$.

The conductivity data was collected using the In-situ Measurement of Porosity (IMP2) system.[9] This system uses a single constant-current electrode that is scanned through the sediment in a 2D plane using a horizontal and vertical positioning system mounted on a frame that rests on the seafloor. The probe can be inserted 25 cm into the sediment in 1 mm increments and at 1 cm horizontal steps up to 4 m. At each position the output voltage of the probe is recorded which is inversely proportional to the mean conductivity over the resolution cell of the electrode. The "formation factor," F, is typically found by taking the ratio of the voltage measured in the sediment to the voltage measured in the overlying water. From the formation factor, the sediment porosity is calculated according to an empirical relation known as Archie's Law,

$$\beta = \frac{1}{F^{1/m}} \tag{1}$$

where m is a constant for a given sediment. This constant is determined by calibrating the probe using a sediment sample that is later dried and weighed to determine the bulk porosity. The spatial distribution of the porosity fluctuations can then be calculated and, if the sediment material properties are known, the density fluctuations can also be calculated. These are used to determine the fluctuation power spectrum, which is used as an input to perturbation theory for volume scattering from the sediment.

An example of the formation factor measured at the BayEx14 site is shown in Figure 2(a). The mud layer (light blue) is clearly resolved by the conductivity probe and has a thickness of $H_{mud} = 13.4 \pm 1.6$ cm, determined from this and other probe measurements at the site. The conductivity probe data also indicates the locations of the mud/water and sand/mud boundaries, from which the 1D roughness power spectra can be calculated as shown in Figure 2(b). The sand/mud boundary is significantly rougher than the mud/water boundary by 10–20 dB in spectral level and roughly 5 dB higher than the roughness measured for typical sand sediments. It's not clear what mechanism produces the

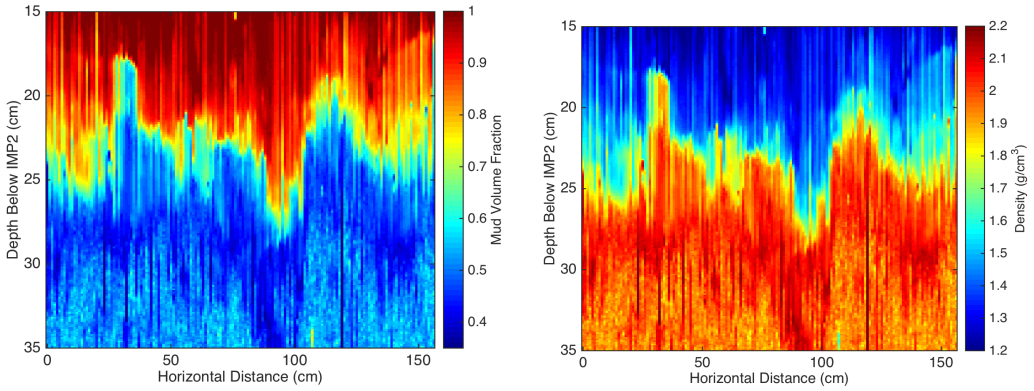

(a) (b)

Figure 3: (a) Mud volume fraction across the sand/mud interface. (b) The sediment density across the sand/mud interface.

roughness at this boundary, but it is likely that the mud preserves the roughness from feeding fish, slumping, and hydrodynamic actions.

The boundary between the mud and sand is also not as sharp as the mud/water boundary. This indicates that the sediment is actually a mix of mud and sand, the ratio of which changes as the boundary is crossed, and suggests an alternative approach to interpreting the formation factor. The particle size in the solid component of the mud is much smaller than the size of the sand grains, $a_{mud} \ll a_{sand}$. It seems reasonable, given the nature of the sediment, to assume that the mud permeates the pores between the sand grains. If the density of the mud is

$$\rho_m = \beta_m \rho_f + (1 - \beta_m)\, \rho_{mg}, \tag{2}$$

where β is the porosity of the mud, ρ_f is the density of the fluid, and ρ_{mg} is the density of the solid component of the mud, then the density of the sediment can be written as

$$\rho = \Phi \rho_m + (1 - \Phi)\, \rho_{sg}, \tag{3}$$

where Φ is the volume fraction of the mud and ρ_{sg} is the density of the sand grains. Using (2) and (3), the actual porosity or volume fraction of water at any point in the sediment is $\beta = \Phi \beta_m$.

To analyze the conductivity probe data, recall that the voltage, V, measured by the probe is inversely proportional to the mean conductivity σ over the resolution cell of the electrode,

$$V = \frac{I}{4\pi\sigma a}, \tag{4}$$

where I is the system current and a is the radius of the probe. Assuming that the conductivity of the mud does not change within the pores of the sediment, we can define a new formation factor as

$$F = \frac{\sigma_m}{\sigma\,(\mathbf{r})} = \frac{V\,(\mathbf{r})}{V_m}, \tag{5}$$

where σ_m and $\sigma\,(\mathbf{r})$ are the conductivities in mud and at position **r** and where V_m and $V\,(\mathbf{r})$ are the voltages in mud and at position **r**. With this definition of the formation factor, we can now use Archie's law to determine the mud volume fraction,

$$\Phi = \frac{1}{F^{1/m}}. \tag{6}$$

This assumes that the Archie's law relationship is valid across the full range of mud volume fractions (0.4– 1.0).

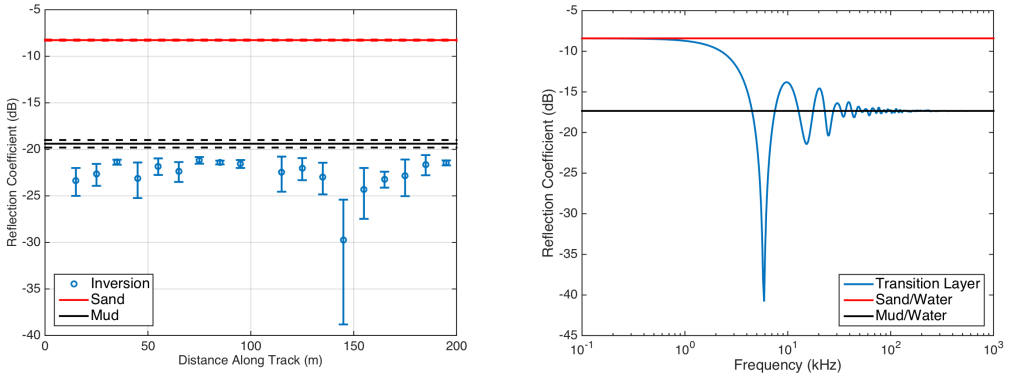

(a) (b)

Figure 4: (a) Normal incidence reflection measured from the sand/mud interface compared to the expected reflection coefficients for a mud/water and a sand/mud interface. (b) Model result for normal incidence reflection from the density profile shown in Fig. 5.

To apply this to BayEx14 conductivity probe data, the formation factor is recalculated by taking the voltage values at 15 cm, where the mud voltages are fairly stable, and divide all of the voltages by these values. Using the porosity values measured using the diver cores in mud and the sand, the mean mud volume fraction in the sand is $\Phi = \beta_s/\beta_m = 0.49$. Using this value and the mean of all formation factor values that are deeper then 30 cm, $m = 0.49$ can be found from Archie's law. The mud volume fraction can now be calculated across the boundary (Figure 3(a)) and from this, using (3), the sediment density can also be found (Figure 3(b)).

The assumption that the mud permeates the pores in the sand layer is consistent with observations made by divers at the site and with visual inspections of the diver cores however it remains to be confirmed by a quantitative analysis of diver cores from the site.

3 DATA/MODEL COMPARISONS

As discussed in Section 2.1, a number of sediment properties are determined by the MBES algorithm. In this paper, we will focus on two of the inversion outputs: the reflection coefficient and the volume scattering cross section.

3.1 NORMAL REFLECTION

The inversion algorithm makes a number of simplifying assumptions about the structure of the sediment in order to limit the number of parameters over which one must search. One of these assumptions, which the BayEx14 sediment violates, is that the sediment can be treated as a half-space. As a result, while the signal reflected from the sediment shows a weak initial return from the mud and a second, stronger return from the sand, the algorithm chooses the larger of the two and assumes that it is the return from the half-space. Since it uses the signal scattered from the sand/mud interface, it is reasonable to expect that the reflection coefficient determined from that signal should correspond to that interface. As can be seen in Figure 4(a), the opposite occurs: the reflection coefficient more closely matches that of the mud/water interface.

To understand why this might be the case, it is necessary to take into account the transition layer at the sand/mud boundary.[10] To determine how the density and sound speed vary across this boundary, the roughness of this boundary is first removed by realigning the vertical profiles such that the interface is flattened as in Figure 5. Once this has been done, the mean density and, through a similar procedure,

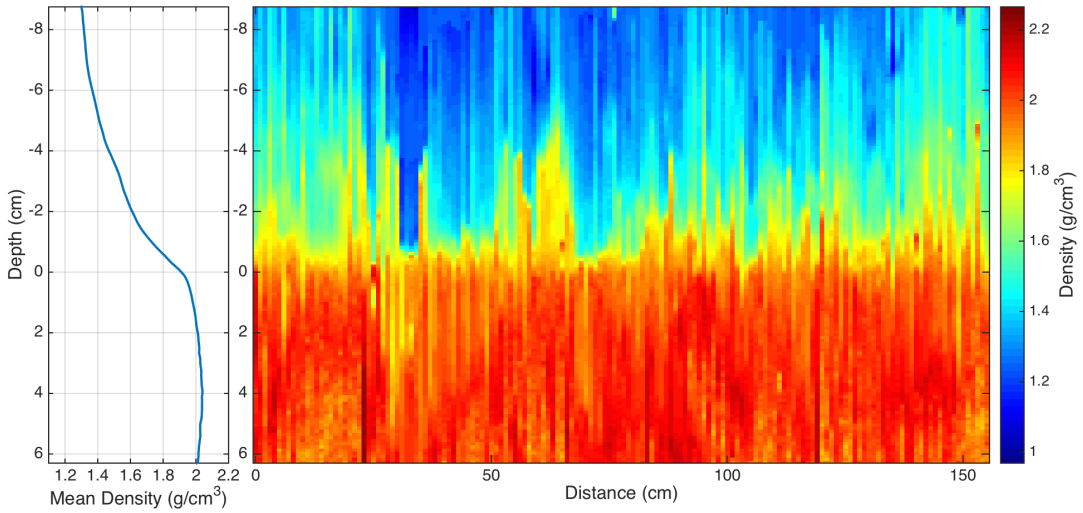

Figure 5: Sediment Density after each vertical density profile has been shifted such to remove the roughness at the sand/mud interface. The left plot shows the mean density across this realigned interface.

the mean sound speed as a function of depth can be found. This profile can be approximated as a sequence of very thin layers for which the reflection coefficient can be determined.[11] The results of this calculation are shown as a function of frequency in Figure 4(b).

At low frequencies, the reflection coefficient corresponds to that of a sand/water interface. As the frequency increases and the wavelength approaches the thickness of the layer, the reflection coefficient decreases and reaches a strong minimum value when the thickness is approximately a quarter wavelength. Beyond this, the reflection coefficient approaches the mud/water value at high frequencies. This occurs since the density is changing at scales much larger than a wavelength and as a result the wave passes smoothly through the boundary. The only reflection therefore occurs at the top of the layer. The reflection values are actually slightly lower than the mud/water value and this is likely due to the small transition layer at the mud/water interface that can be seen in Figure 2(a) but is not accounted for in the model. Also, in using the profile in Fig. 5, the model assumes a constant thickness for the mud layer. As indicated in Fig. 2(a), the thickness of the layer varies with location and this will have the effect of smoothing the low to high frequency transition, removing the the strong nulls in the reflection coefficient.

3.2 VOLUME SCATTERING

The volume scattering strength determined by the inversion algorithm is shown in Figure 6(b). The algorithm again treats the sediment as a half-space and assumes that the volume scattering cross section is constant throughout the half space. Shown in the figure are two different results; the first assumes that the sand/mud boundary is abrupt while the second assumes that it has the profile shown in Figure 5. This slightly lowers the volume scattering strength (~ 1 dB).

To model the scattering strength, the density data shown in Figure 2(b) is used to determine the density fluctuations in the sand sediment sediment. Using several IMP2 data sets from different locations, the resulting 1D power spectra are shown in Figure 6(a). These are converted to 3D spectra and used in the small perturbation scattering approximation.[12] The model results are compared to the inversion in Figure 6 where they underpredict the inversion results by 5–10 dB.

One possibility for this discrepancy is that since the interface is very rough and sitting in the transition layer, it becomes difficult to discriminate between interface scattering and volume scattering along

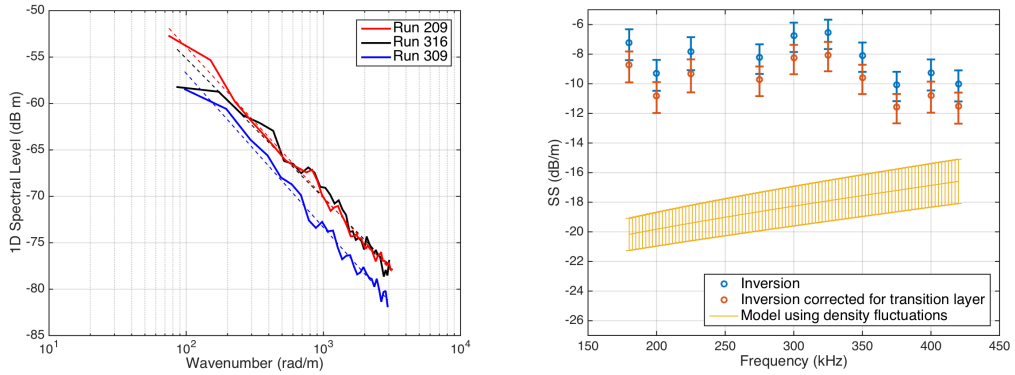

(a) (b)

Figure 6: (a) Heterogeneity spectrum measured in the sand layer. (b) The volume scattering strengths determined from the inversion compared to the small perturbation approximation predictions.

this interface since the boundary is no longer clear. The inversion may be treating this interface as volume scattering where the scattering based on the density fluctuations is not taking this into account. This hypothesis is also consistent with spectral inversions of the roughness scattering strength where the inversion slightly under estimates the sand/mud interface roughness spectrum. This is also supported by inversions that were performed using a more complex model. This model estimates volume scattering strengths for two regions, a 15 cm layer starting at the sand/mud interface and the half space below. This half space contains the regions in which the heterogeneity was measured. For the more complicated inversions, volume scattering strengths for the 15 cm layer are similar to those obtained from the simpler inversion, but those for the lower half-space agree with ground-truth within measurement uncertainties. Thus, the inversion agrees with ground truth when it isolates the region in which the ground-truth measurements were made.

4 CONCLUSIONS

The BayEx14 site, like many sediments, has a deceptively simple description: a 13 cm mud layer over a sand bottom. Using a conductivity probe which could measure the density profile in 2D planes through the mud layer and into the sand, this “simple” sediment was found to have a level of complexity that, if not accounted for, would lead to erroneous conclusions about the nature of the acoustic interactions. This was seen in both the data/model comparisons for the normal incidence reflection coefficient and for the scattering strengths. In the first case, the reflection model needed to account for the transition layer at the sand/mud boundary and, for the volume scattering, the inversion needed to be modified to take into account the ambiguous nature of the scattering at the transition layer. An alternative may be to use a unified approach to modeling the scattering at the boundary such as that developed in Ref. 13.

5 ACKNOWLEDGEMENTS

This work was supported by the Strategic Environmental Research and Development Program and the US Office of Naval Research. The authors would also like to thank Dr. Gorm Wendelboe and Teledyne-RESON for providing the multibeam sonar and the technical assistance necessary for its deployment.

6 REFERENCES

1. E. I. Thorsos, K. L. Williams, N. P. Chotiros, J. Christoff, K. Commander, C. Greenlaw, D. Holliday, D. R. Jackson, J. Lopes, D. McGehee, J. Piper, M. Richardson, and D. Tang. An overview of SAX99: acoustic measurements. *IEEE J. of Ocean. Eng.*, 26(1): pp. 4–25, (2001).

2. K. L. Williams, D. R. Jackson, D. Tang, K. B. Briggs, and E. I. Thorsos. Acoustic Backscattering From a Sand and a Sand/Mud Environment: Experiments and Data/Model Comparisons. *IEEE J. of Ocean. Eng.*, 34(4): pp. 388–398, (2009).

3. B. T. Hefner and D. Tang. Overview of the reverberation component of TREX13. In *Proceedings of the 2nd International Conference and Exhibition on Underwater Acoustics, 22-27 June*, Rhodes, Greece, (2014).

4. D. R. Jackson, B. T. Hefner, A. N. Ivakin, and G. Wendelboe. Seafloor characterisation using physics-based inversion of multibeam sonar data. In *Proceeding of the 11th European Conference on Underwater Acoustics*, pp. 1571–1576, (2012).

5. E. Pouliquen and X. Lurton. Seabed identification using echo-sounder signals. *ECUA 1992*, : pp. 535–538, (1992).

6. D. D. Sternlicht and C. P. de Moustier. Time-dependent seafloor acoustic backscatter (10-100 kHz). *J. Acoust. Soc. Am.*, 114: pp. 2709–2725, (2003).

7. D. D. Sternlicht and C. P. de Moustier. Remote sensing of sediment characteristics by optimized echo-envelope matching. *J. Acoust. Soc. Am.*, 114: pp. 2727–2743, (2003).

8. C. De and B. Chakraborty. Acoustic characterization of seafloor sediment employing a hybrid method of neural network architecture and fuzzy algorithm. *Geoscience and Remote Sensing Letters, IEEE*, 6(4): pp. 743–747, (2009).

9. D. Tang. Fine-scale measurements of sediment roughness and subbottom variability. *IEEE J. of Ocean. Eng.*, 29: pp. 929–939, (2005).

10. A. Lyons and T. H. Orsi. The effect of a layer of varying density on high-frequency reflection, forward loss, and backscatter. *IEEE J. of Ocean. Eng.*, 23(4): pp. 411–422, October (1998).

11. L. M. Brekhovskikh and I. U. P. Lysanov. *Fundamentals of Ocean Acoustics*. Modern Acoustics and Signal Processing. Springer, (2003).

12. D. R. Jackson and M. Richardson. *High-Frequency Seafloor Acoustics*. Springer, New York, NY, (2006).

13. A. Ivakin. Unified approach to volume and roughness scattering. *J. Acoust. Soc. Am.*, 103(2): pp. 827–837, (1998).